Available online at www.sciencedirect.com
ScienceDirect
Nuclear and Particle Physics Proceedings 00 (2016) 1–4
Nuclear and Particle Physics Proceedings

Leading Hadron Production in d+Au and ^{3}He+Au collisions in the PHENIX experiment

Takao Sakaguchi, for the PHENIX collaboration

Physics Department, Brookhaven National Laboratory, Upton, NY 11973, USA

arXiv:1612.06894v1 [nucl-ex] 20 Dec 2016

Abstract

Neutral pions have been measured in ^{3}He+Au collisions at $\sqrt{s_{NN}}$=200 GeV up to 20 GeV/c in the RHIC Year-2014 run. The nuclear modification factor $R_{\rm AA}$ was measured and compared with that from d+Au collisions. The integrated $R_{\rm AA}$ as a function of $N_{\rm part}$ was calculated for d+Au, ^{3}He+Au and Au+Au collisions at $\sqrt{s_{NN}}$=200 GeV, and found to converge for $N_{\rm part}$ >12, while a clear system ordering $R_{\rm dAu}$>$R_{\rm HeAu}$>$R_{\rm AuAu}$ was observed for $N_{\rm part}$ <12. The fractional momentum loss for the most central ^{3}He+Au collisions was also estimated.

Keywords:

1. Introduction

The small collision systems such as p/d+A collisions have been considered a good laboratory to quantify cold nuclear matter effects, a necessary baseline for understanding the effects of the hot and dense medium produced in A+A collisions. The observation of the ridge-like structure in the long-range azimuthal correlations in p+Pb collisions at $\sqrt{s_{NN}}$=5.02 TeV at the LHC [1, 2], however, called into question the view of such systems as consisting merely of cold nuclear matter. The study at the LHC was followed by the PHENIX experiment at RHIC, and a finite v_2 of hadrons in 0–5 % central d+Au collisions using both the two-particle angular correlation method and the event-plane method were shown [3, 4]. These observations led the community to explore any phenomena found in A+A collisions, in p/d+A collisions.

The energy loss of hard scattered partons produced in the initial stage of the collisions, so-called jet quenching, has been one of the key observations in confirming the production of the QGP. The first evidence of this phenomena was found in the yield suppression of high transverse momentum ($p_{\rm T}$) hadrons, the fragments of the hard scattered partons. The measurement of high $p_{\rm T}$ identified hadrons have been improved over the last decade, and reached to the level that a precise quantitative comparison of the data and theoretical models became realized [5, 6]. A recent study also found that the energy loss scales with the particle multiplicity ($dN/d\eta$) [7]. Obviously, the high $p_{\rm T}$ hadrons will be a powerful tool to investigate the parton degree of freedom in the small systems like p/d+A collisions as well. In addition, a systematic study of the high $p_{\rm T}$ hadron spectra from small to large collision systems will be able to explore the onset of QGP as a function of the collision systems. In this paper, we show the new measurement of the high $p_{\rm T}$ π^0 in ^{3}He+Au collisions and compared with the ones from d+Au and Au+Au collisions and discuss the systematics of the yield suppression and enhancement of the high $p_{\rm T}$ hadrons.

2. Detector and Dataset

PHENIX recorded an integrated luminosity of 25 nb^{-1} in ^{3}He+Au collisions at $\sqrt{s_{NN}}$=200 GeV in the RHIC Year-2014 run. The detector setup was the same as the one in the RHIC Year-2012 run as shown in Fig. 1. The detailed description of the PHENIX detector system can be found elsewhere [8]. The π^0 was

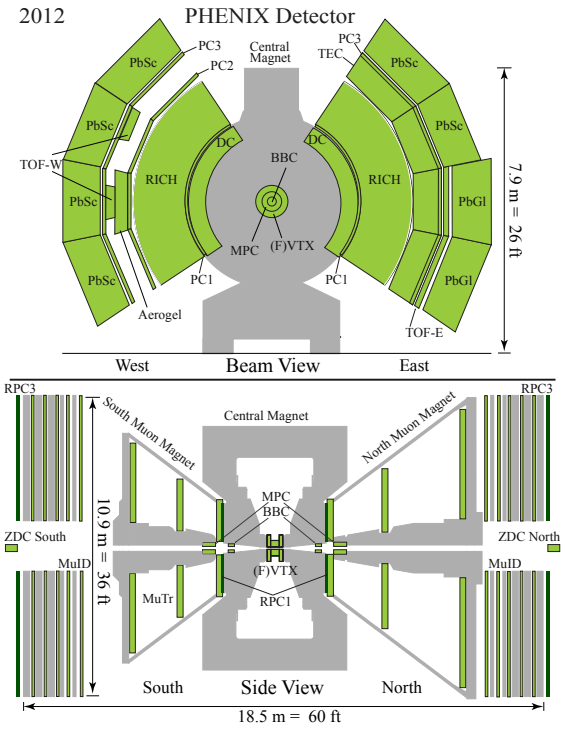

Figure 1: PHENIX detector setup in the RHIC Year-2014 run.

reconstructed via $\pi^0 \rightarrow \gamma\gamma$, by primarily using a lead-scintillator sandwich type electromagnetic calorimeter (PbSc EMCal). The threshold of cluster energy is set to 0.2 GeV and the photon clusters were selected using a shower shape cut. Then, an energy asymmetry cut of $\alpha = |E_1 - E_2|/(E_1 + E_2) < 0.8$ was applied on selecting pairs of photons from π^0 decay. The efficiency and acceptance of the π^0 were estimated using a GEANT-based detector simulation software.

Two types of the trigger selections were used to trigger events; one is the coincidence of the signals from the two Beam-Beam counters (BBC) located at $3.1 < |\eta| < 3.9$ covering the full azimuth (minimum bias trigger), and the other is the coincidence of the minimum bias trigger and a high energy tower hit in the EMCal (ERT trigger). The events we used in this analysis were 2×10^9 minimum bias triggered events, and 4.5×10^{10} minimum-bias-equivalent ERT events, totaling in the integrated luminosity of 22 nb^{-1}. The minimum bias trigger is not 100 % efficient to the inelastic collisions because of the limited acceptance and efficiency of the BBC. This inefficiency increases as the collision system becomes smaller. They were already studied in d+Au collisions by comparing the BBC charge with a Glauber Monte Carlo simulation folded with a negative binomial distribution [9]. From this comparison, we determined that the trigger efficiency is 88 % for d+Au collisions. We followed the same method, and determined the trigger efficiency of ^{3}He+Au collisions also as 88 %. In case of 200 GeV Au+Au collisions, the efficiency was 94 %. When dividing the events into centralities, an additional bias factor plays a role. The bias is originated from the anti-correlation of the available energies for producing particles in midrapidity where the EMCal is installed, and the backward rapidity where the BBC sits. We estimated the bias factors for the ^{3}He+Au collisions, also by following the method used for d+Au collisions, and determined as 0.95, 1.02, 1.02, 1.03, and 0.89 for 0–20, 20–40, 40–60, 60–88, and 0–100 % ^{3}He+Au collisions, respectively [9]. We divided uncorrected yields by these factors.

3. Results

Fig. 2 shows the invariant spectra of the π^0 as a function of p_T in ^{3}He+Au collisions at $\sqrt{s_{NN}}$=200 GeV. The

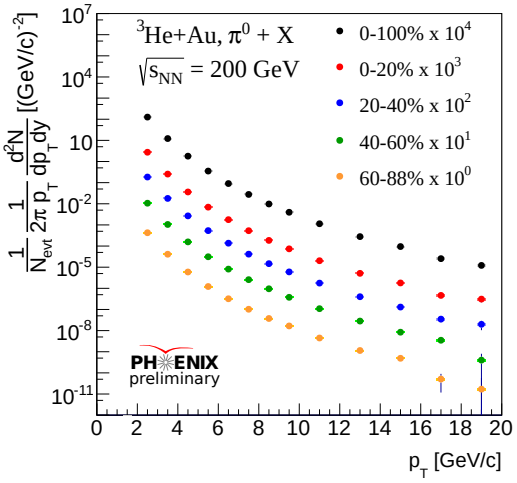

Figure 2: Invariant p_T spectra of π^0 in ^{3}He+Au collisions at $\sqrt{s_{NN}}$=200 GeV.

spectra from the minimum bias triggered events and the ERT triggered events were connected at p_T =6 GeV/c. The spectra were successfully measured in the four centrality classes (0–20, 20–40, 40–60, and 60-88 %) as well as the minimum bias events, up to p_T =20 GeV/c. The spectra are in a power-law shape suggesting that the dominant source is the initial hard scattering. In order to quantify the spectra change with respect to the one from

the primordial production (p + p collisions), we computed the nuclear modification factor ($R_{\rm AA}$) for all the five event classes. We used the π^0 spectra from the $p+p$ collisions measured in the RHIC Year-2005 run as the baseline [10]. Fig. 3 shows the $R_{\rm AA}$ for the minimum bias ^{3}He+Au collisions. The $R_{\rm AA}$ for the minimum bias

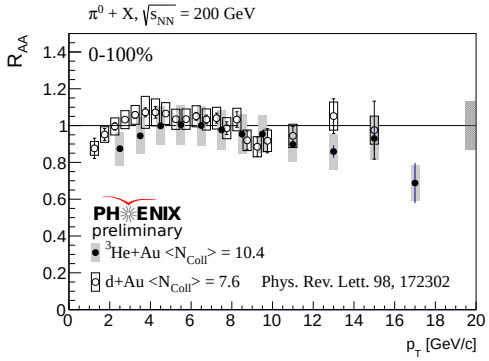

Figure 3: $R_{\rm AA}$ for 0–100 % ^{3}He+Au collisions with the one from d+Au collisions.

d+Au collisions measured in RHIC Year-2003 run are also shown for comparison [11]. In both systems, the $R_{\rm AA}$'s are consistent with unity within quoted uncertainties. In Figs. 4, 5, 6, and 7, $R_{\rm AA}$'s for 0–20, 20–40, 40–60, 60–88 % ^{3}He+Au collisions are shown, again together with the ones in d+Au collisions, respectively.

The magnitude and the $p_{\rm T}$ dependence of the $R_{\rm AA}$ in

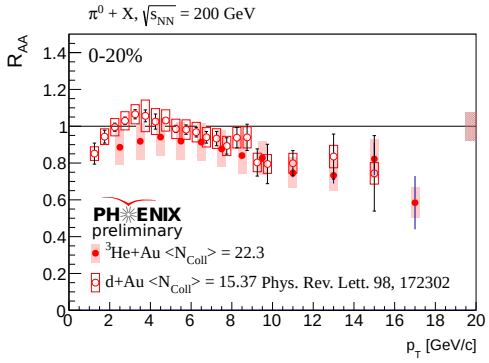

Figure 4: $R_{\rm AA}$ for 0–20 % ^{3}He+Au collisions with the one from d+Au collisions.

the both systems are remarkably similar within quoted uncertainties for all the centrality classes. However, a small systematic difference is seen, especially at the low $p_{\rm T}$ region ($p_{\rm T}$ <5 GeV/c).

In order to systematically compare the enhancement/suppression of the invariant yields in two systems,

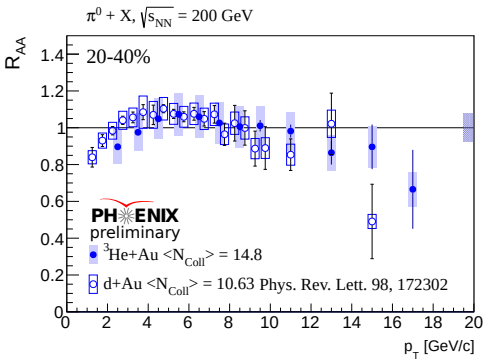

Figure 5: $R_{\rm AA}$ for 20–40 % ^{3}He+Au collisions with the one from d+Au collisions.

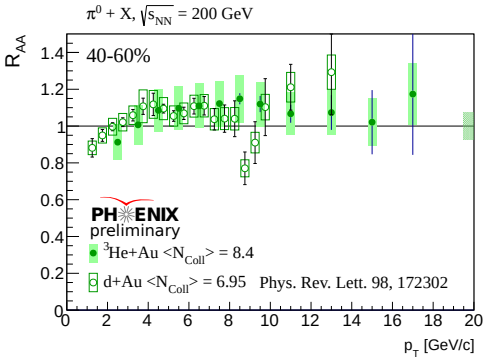

Figure 6: $R_{\rm AA}$ for 40–60 % ^{3}He+Au collisions with the one from d+Au collisions.

we plotted the integrated $R_{\rm AA}$ for ^{3}He+Au and d+Au collisions as a function of number of participant nucleons ($N_{\rm part}$) as shown in Fig. 8.

The integrated $R_{\rm AA}$ for three $p_{\rm T}$ ranges, namely $p_{\rm T}$ >5 GeV/c, >8 GeV/c, and >10 GeV/c, agree each other for all the points, suggesting that the $R_{\rm AA}$ is flat over $p_{\rm T}$ within the quoted uncertainties. At the higher $N_{\rm part}$, the d+Au and ^{3}He+Au collisions show the very similar $N_{\rm part}$ dependence, while at the lower $N_{\rm part}$, a clear distinction between two collision systems are seen; the ones in d+Au collisions show larger enhancement, suggesting a larger Cronin effect or less suppression (energy loss). We can study the trend even more systematically by comparing those with the $R_{\rm AA}$'s from the peripheral Au+Au collisions, i.e., 60–70, 70–80, and 80–93 % centrality. In the previous publication, we measured the $R_{\rm AA}$ for $p_{\rm T}$ >5 GeV/c as ~0.78, ~ 0.87, and ~0.84, for $N_{\rm part}$ of 26.7±3.7, 13.7±2.5, and 5.6±0.8, respectively [6]. From these numbers, we found that the $R_{\rm AA}$'s from the three collisions systems

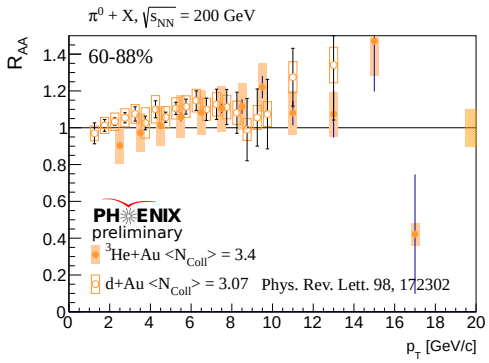

Figure 7: $R_{\rm AA}$ for 60–88 % ^{3}He+Au collisions with the one from d+Au collisions.

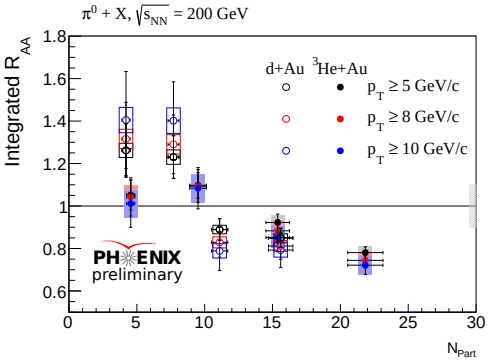

Figure 8: Integrated $R_{\rm AA}$ for d+Au and ^{3}He+Au collisions.

converge for $N_{\rm part}$ >12, while a system ordering of $R_{\rm dAu}$>$R_{\rm HeAu}$>$R_{\rm AuAu}$ is observed for $N_{\rm part}$ <12. The uncertainty needs to be improved in order to make a concrete statement, but this finding suggests that a similar medium, possibly a hot dense medium, may be created for the system for $N_{\rm part}$ >12. Lastly, by comparing with the detail study of the fractional momentum loss ($\delta p_{\rm T}/p_{\rm T}$) in Au+Au collisions carried out in the previous publication, we found the most central ^{3}He+Au collisions exhibit $\delta p_{\rm T}/p_{\rm T}$ ~0.03 [7].

4. Summary

Identified π^0 has been measured in ^{3}He+Au collisions at $\sqrt{s_{NN}}$=200 GeV in the RHIC Year-2014 up to 20 GeV/c in four centrality classes as well as in the minimum bias events. The $R_{\rm AA}$ was computed and compared with those from d+Au collisions, and found that they are consistent with quoted uncertainties, however, small difference was seen between two systems, especially at the low $p_{\rm T}$. The integrated $R_{\rm AA}$ from d+Au, ^{3}He+Au and Au+Au collisions at $\sqrt{s_{NN}}$=200 GeV were found to converge for $N_{\rm part}$ >12, while a clear system ordering $R_{\rm dAu}$>$R_{\rm HeAu}$>$R_{\rm AuAu}$ was observed for $N_{\rm part}$ <12, suggesting a similar medium may be created for the system for $N_{\rm part}$ >12. We also found the most central ^{3}He+Au collisions exhibited $\delta p_{\rm T}/p_{\rm T}$ ~0.03. The measurement in p+Au collisions at RHIC will help completing this systematic study and could point the onset of QGP in terms of the collision system size.

References

[1] G. Aad, et al., Observation of Associated Near-Side and Away-Side Long-Range Correlations in $\sqrt{s_{NN}}$=5.02 TeV Proton-Lead Collisions with the ATLAS Detector, Phys. Rev. Lett. 110 (18) (2013) 182302. arXiv:1212.5198, doi:10.1103/PhysRevLett.110.182302.

[2] G. Aad, et al., Measurement of long-range pseudorapidity correlations and azimuthal harmonics in $\sqrt{s_{NN}}$ = 5.02 TeV proton-lead collisions with the ATLAS detector, Phys. Rev. C90 (4) (2014) 044906. arXiv:1409.1792, doi:10.1103/PhysRevC.90.044906.

[3] A. Adare, et al., Quadrupole Anisotropy in Dihadron Azimuthal Correlations in Central d+Au Collisions at $\sqrt{s_{NN}}$=200 GeV, Phys. Rev. Lett. 111 (21) (2013) 212301. arXiv:1303.1794, doi:10.1103/PhysRevLett.111.212301.

[4] A. Adare, et al., Measurement of long-range angular correlation and quadrupole anisotropy of pions and (anti)protons in central d+Au collisions at $\sqrt{s_{NN}}$=200 GeV, Phys. Rev. Lett. 114 (19) (2015) 192301. arXiv:1404.7461, doi:10.1103/PhysRevLett.114.192301.

[5] A. Adare, et al., Quantitative Constraints on the Opacity of Hot Partonic Matter from Semi-Inclusive Single High Transverse Momentum Pion Suppression in Au+Au collisions at $\sqrt{s_{NN}}$ = 200-GeV, Phys. Rev. C77 (2008) 064907. arXiv:0801.1665, doi:10.1103/PhysRevC.77.064907.

[6] A. Adare, et al., Neutral pion production with respect to centrality and reaction plane in Au+Au collisions at $\sqrt{s_{NN}}$=200 GeV, Phys. Rev. C87 (3) (2013) 034911. arXiv:1208.2254, doi:10.1103/PhysRevC.87.034911.

[7] A. Adare, et al., Scaling properties of fractional momentum loss of high-p_T hadrons in nucleus-nucleus collisions at $\sqrt{s_{NN}}$ from 62.4 GeV to 2.76 TeV, Phys. Rev. C93 (2) (2016) 024911. arXiv:1509.06735, doi:10.1103/PhysRevC.93.024911.

[8] K. Adcox, et al., PHENIX detector overview, Nucl. Instrum. Meth. A499 (2003) 469–479. doi:10.1016/S0168-9002(02)01950-2.

[9] A. Adare, et al., Centrality categorization for $R_{p(d)+A}$ in high-energy collisions, Phys. Rev. C90 (3) (2014) 034902. arXiv:1310.4793, doi:10.1103/PhysRevC.90.034902.

[10] A. Adare, et al., Inclusive cross-section and double helicity asymmetry for π^0 production in p + p collisions at $\sqrt{s_{NN}}$ = 200-GeV: Implications for the polarized gluon distribution in the proton, Phys. Rev. D76 (2007) 051106. arXiv:0704.3599, doi:10.1103/PhysRevD.76.051106.

[11] S. S. Adler, et al., Centrality dependence of π^0 and η production at large transverse momentum in $\sqrt{s_{NN}}$ = 200-GeV d+Au collisions, Phys. Rev. Lett. 98 (2007) 172302. arXiv:nucl-ex/0610036, doi:10.1103/PhysRevLett.98.172302.